N89-24972

SIMULATION OF ELECTROSTATIC ION INSTABILITIES IN THE PRESENCE OF PARALLEL CURRENTS AND TRANSVERSE ELECTRIC FIELDS

K-I Nishikawa*, G Ganguli, †Y C Lee** & P J Palmadesso*****

**Dept. of Physics & Astronomy, The University of Iowa, IO*
***Science Applications International Corporation, McLean, VA*
****Plasma Physics Division, Naval Research Laboratory, Washington, DC, USA*

ABSTRACT

Broadband electrostatic turbulence has been observed recently in the auroral regions in conjunction with transverse d.c. electric fields. Generally, field-aligned electron drifts are also found in this region. Using a spatially two-dimensional electrostatic PIC simulation code, we have studied the stability of a plasma equilibrium characterized by a localized transverse d.c. electric field and and a field-aligned drift for $L \ll L_x$, where L_x is the simulation length in the x direction and L is the scale length associated with the d.c. electric field. It is found that the d.c. electric field and the field-aligned current can together play a synergistic role to enable the excitation of electrostatic waves even when the threshold values of the field aligned drift and the $\mathbf{E} \times \mathbf{B}$ drift are individually subcritical. The simulation results show that the growing ion waves are associated with small vortices in the linear stage, which evolve to the nonlinear stage dominated by larger vortices with lower frequencies.

Keywords: Parallel Currents, Transverse Electric Fields, Inhomogeneous Energy Density Driven Instability, Vortices, $\mathbf{E} \times \mathbf{B}$ drift, Anomalous Diffusion.

1. INTRODUCTION

Recently, shears in the transverse flow velocity and associated broadband electrostatic turbulence have been observed in a wide range of the auroral region (Ref. 1-5). Basu *et al.* (Ref. 2,3) using DE 2 satellite data and Earle (Ref. 4) using COPE rocket data provide clear evidence of strong velocity shears (10 to 25Hz) and associated broadband fluctuations in the auroral F region. Besides the shear in the transverse flow velocity, a magnetic field-aligned current (FAC) also exists in this region. Generally the observed magnitudes of the FAC are below the threshold value necessary for the excitation of the Current Driven Ion Cyclotron Instability (CDICI) as described by Drummond and Rosenbluth (Ref. 6).

Ganguli et al. have developed a kinetic theory (Ref. 7,8) to explain the electrostatic waves associated with transverse velocity shears. Recently the initial kinetic theory (Ref. 7,8) has been generalized to include continuous gradients in the d.c. electric field. In the weak shear limit (i.e $V_E'(x)/\Omega_i \ll 1$, where V_E' is the spatial derivative of the $\mathbf{E} \times \mathbf{B}$ drift and Ω_i is the ion cyclotron frequency), the distinctions between the Inhomogeneous Energy Density Driven Instability (IEDDI) and the kinetic K-H instability have been studied. The growth rates of the kinetic K-H modes were obtained for various values of $u = k_{\|}/k_y$ where $k_{\|}$ and k_y are the components of the wave vector in the z (parallel to the magnetic field B) and the y directions. It was found that the K-H mode is localized below $b = k_y^2\rho_i^2 = 1$ and $k_yL \sim 1$, where L is the scale length associated with the d.c. electric field and $\rho_i = v_i/\Omega_i$ is the ion gyro-radius. Furthermore, the growth rates are reduced strongly as u increases. The growth rates for the IEDDI were also obtained. This mode becomes unstable where $b \gg 1$ and $k_yL \gg 1$. The unstable domains for both modes are distinct.

Nishikawa *et al.* (Ref. 10) investigated the IEDDI by means of particle simulations. The linear analysis of waves obtained from the simulations show that the mode (0, 4) which corresponds to $b = 3.38$ and $k_yL = 4.31$ has the maximum growth rate and falls on the IEDDI branch. The emphasis in this simulation (Ref. 10) was to demonstrate the existence of the new mode (IEDDI) and distinguish it from the well-known Kelvin-Helmholtz branch and the kinetic modification of this branch.

Subsequently, Ganguli and Palmadesso (Ref. 11) and Ganguli *et al.* (REF. 12) have shown that the simultaneous existence of transverse localized electric (TLE) fields and field-aligned currents (FAC) can excite electrostatic waves even though the electric field and the current are individually subcritical. In the presence of TLE fields, the Doppler shift due to the $\mathbf{E} \times \mathbf{B}$ drift plays an important role and the threshold value of the FAC for exciting the CDICI is effectively lowered (Ref. 12). The character of the waves depend on R $(= k_yV_E/k_zV_d)$, the ratio of the Doppler shifts due to the

† Permanent address: University of Maryland, College Park, Maryland 20742

Proceedings of the Joint Varenna-Abastumani International School & Workshop on Plasma Astrophysics, held in Varenna, Italy, 24 Aug.–3 Sept. 1988 (ESA SP-285, Vol. I, Dec. 1988).

drifts originating from the TLE and the FAC. For $R < 1$ the waves are CDICI-like while for $R > 1$ the waves are IEDDI-like.

Here we describe the numerical simulations that have been performed in order to understand the excitation of electrostatic waves in the simultaneous presence of a field-aligned electron drift and a transverse d.c. electric field (Ref. 12) and it's evolution to the nonlinear regime. In Sec. II. the simulation model and results are presented and concluding remarks and discussions are described in Sec. III.

2. SIMULATION MODEL AND RESULTS

A two-dimensional electrostatic code is used which retains the full dynamics of the ions in three dimensional velocity space. Electrons are treated by the guiding center approximation in the perpendicular direction while the parallel motion is treated exactly. We use a system length $L_x = 128\Delta$, $L_y = 32\Delta$, where Δ is the grid size which is equal to the electron Debye length, λ_e and $\overline{n}_e\lambda_e^2 = 36$. In the previous work (Ref. 10), we found that the IEDDI has the maximum growth rate around $k_y\rho_i = 1.84$ which corresponds to (0, 2) mode in the case of $L_y = 32\Delta$. By using the system length $L_y = 32\Delta$ instead of 64Δ, we can isolate only the IEDDI (Ref. 10) by cutting out the KH instability from the system. The external electric field is applied in the form of $E_{ox}(x) = E_{ox}\mathrm{sech}^2[(x-64)/L_v]$ in the x direction which produces $\mathbf{E}\times\mathbf{B}$ drift in the y direction given by $V_E(x) \simeq -cE_{ox}(x)/B_o$. The parallel electron drifts are initialized in the form of $V_d(x) = V_d^o\mathrm{sech}^2[(x-64)/L_c]$. Here we maintain $L_c = L_v$, but this restriction can easily be relaxed.

For the present problem, in which a nonuniform d.c. electric field transverse to the uniform magnetic field is present, an appropriate initial distribution function has been constructed out of the constants of motion (Ref. 9). For the purpose of initial loading in a computer simulation, the distribution can be expressed in terms of the physical position x (for details see Ganguli *et al.* (Ref. 9)),

$$2\pi f_{0\perp} = \frac{\beta\exp\{-\frac{\beta}{2}[v_x^2 + \frac{(v_y - V_E(x))^2}{\eta(x)}]\}}{\sqrt{\eta(x)}}[1 + O(\epsilon)]. \quad (1)$$

Here $\eta = 1 + V_E'(x)/\Omega_i$ and $v_t = \beta^{-1/2}$ is the thermal velocity. Note that the distortion in the gyro-orbit introduced by the sheared d.c. electric field leads to a sustainable difference in the temperature in the two dimensions transverse to the uniform magnetic field. For weak shears (i.e. $|V_E'/\Omega| \ll 1$), Eq. (1) reduces to,

$$2\pi f_{0\perp} = \beta\{1 + \frac{\beta V_E'(x)}{4\Omega}[(v_y - V_E(x))^2 - v_x^2]\} \times \exp\{-\frac{\beta}{2}[v_x^2 + (v_y - V_E(x))^2]\}.$$

We see that for weak shears the use of a shifted Maxwellian for the initial loading is acceptable and the system will adjust to the above distribution automatically with only minor relaxation (Ref. 10). If the V_E'/Ω correction is ignored, then Eq. (2) becomes identical to a Maxwellian shifted by the magnitude of the $\mathbf{E}\times\mathbf{B}$ drift in the y component of the velocity. This describes the distribution function transverse to the magnetic field. We use $f_{0\|} = (\beta/2\pi)^{1/2}exp(-\beta(v_\| - V_d(x))^2/2)$ as the distribution function along the magnetic field so that $f_0 = f_{0\perp}f_{0\|}$.

We first choose three set of parameters: (i) $V_d^o = -0.4v_e$ and $V_E^o = 0.0$, (ii) $V_d^o = 0.0$ and $V_E^o = 0.15v_i$, and (iii) $V_d^o = -0.4v_e$ and $V_E^o = 0.15v_i$, where V_d^o, V_E^o, v_e and v_i are the peak values of $V_d(x)$ and $V_E(x)$, and the electron and ion thermal velocities, respectively. Other parameters used are $B_{oy}/B_o\,(= k_\|/k_y) = 0.005$, $\Omega_e/\omega_{pe} = 4$, $T_i/T_e = 3.5$, $m_i/m_e = 100$, $\alpha = E_{0x}^2/4\pi n_e T_e = 0.0125$, $\epsilon = \rho_i/L = 0.42$, and $L = L_v = L_c = 11\Delta$. We display in Figure 1 the time evolutions of the fluctuating electrostatic potentials and their corresponding power spectra for the mode (0, 2). The mode (0,2) corresponds to $b = 3.38$, $k_y\rho_i = 1.84$, $k_yL = 4.31$. Here the magnitude of the peak shear $V_E^o/L\Omega_i = 0.063$. Also, since $R = 14 >> 1$, the waves are IEDDI-like.

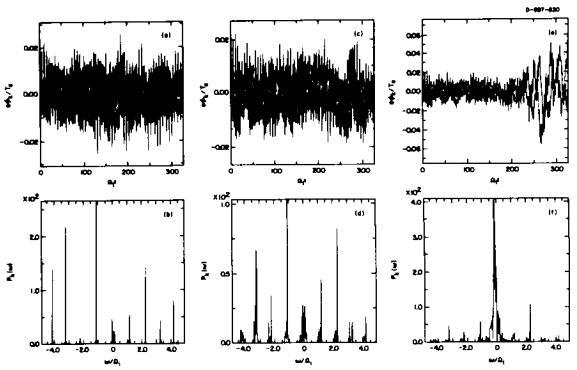

Figure 1. The comparison of the time evolutions and their spectra of the (0, 2) modes among the three cases.
(a) and (b): $V_d^o = -0.4v_e$ and $V_E^o = 0.0$,
(c) and (d): $V_d^o = 0.0$ and $V_E^o = 0.15v_i$,
(e) and (f): $V_d^o = -0.4v_e$ and $V_E^o = 0.15v_i$.

As shown in Figure 1, the cases with only the parallel electron drift (a) or only the transverse electric field (c), cannot sustain any growing wave. In their spectra (Figure 1 (b) and (d)), the thermal noises at the cyclotron frequency and its higher harmonics are observed at low intensity. On the other hand, we see that the combination of the TLE and the FAC can sustain growing waves. The waves begin to grow and emerge from the background thermal noise around $\Omega_i t = 220$ and subsequently reach the nonlinear stage around $\Omega_i t = 300$. As shown in Figure 1 (f), the peak of the frequency spectrum is located around $-0.2\Omega_i$. In Figure 1 (f) we also find a number of smaller peaks around higher harmonics.

In Figure 2 we show the time evolutions of the modes (0,3) and (0,4) ((a) and (c)) and their corresponding power spectra ((b) and (d)). Here rest of the parameters are unchanged from the previous case.

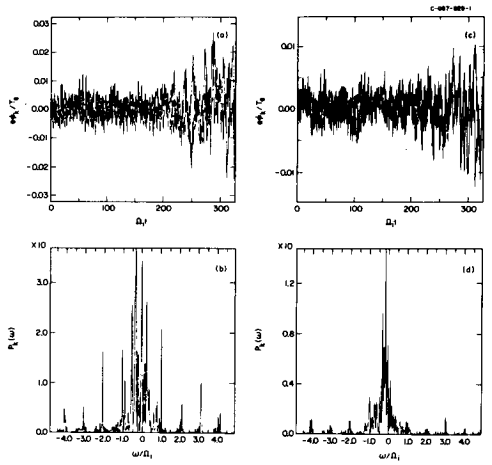

Figure 2. The time evolutions ((a), (c)) and their power spectra ((b), (d)) of perturbations of electrostatic potential for two modes with the parallel currents and the electric fields.
(a) and (b): $k_{\|}\lambda_{e\|} = 0.005 \times 2\pi \times 3/32 = 2.95 \times 10^{-3}$, $k_y\lambda_{e\|} = 2\pi \times 3/32 = 0.589$.
(c) and (d): $k_{\|}\lambda_{e\|} = 0.005 \times 2\pi \times 4/32 = 3.93 \times 10^{-3}$, $k_y\lambda_{e\|} = 2\pi \times 4/32 = 0.785$.

The mode (0, 3) has a peak with the larger real frequency at -0.3Ω_i as shown in Figure 2 (b). It is interesting to note that the power spectra (b and d) are remarkably similar in general features (e.g., spiky nature, generation of higher harmonics etc.) to the high time resolved spectra given by Prikryl et al. (Ref. 13), which were obtained from their radar measurement of the plasma irregularities in the auroral region.

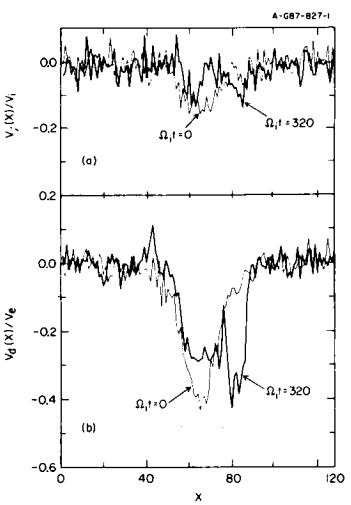

Figure 3. The average ion flow velocity $v_y(x)$ (a) and the parallel electron currents V_d (b) at $\Omega_i t = 0$ and 320.

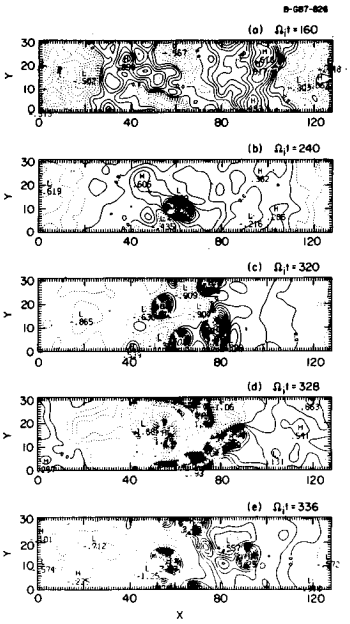

Figure 4. The time evolution of the contour plot of the of the electrostatic potential in the linear stage $\Omega_i t = 160$ and 240, and in the nonlinear stage $\Omega_i t = 320$, 328, and 336.

The average ion flow velocities $V_y(x)$ and average electron flow velocities $V_d(x)$ are shown in Figure 3. In the linear stage ($\Omega_i t < 100$) there is hardly any reduction in the peak of the velocity profile or any relaxation in the topology of the profile. At $\Omega_i t = 320$ (thicker curves), the peaks are moved at $x = 80$ due to nonlinear effects. It should be noted that the value of peak of electron currents remains almost unchanged. On the other hand, in the late quasilinear ($\Omega_i t \simeq 240$) and the nonlinear ($\Omega_i t > 320$) stages the wave amplitude become large and can interact with and reduce the magnitude of the d.c. electric field. In the final stages of the simulation we see a reduction in the magnitude of $V_E(x)$. Since the real frequency is proportional to $k_y V_E(x)$ (see Ganguli *et al.* (Ref. 9)), we find that in the quasilinear stage the real frequency starts reducing along with the magnitude of $V_E(x)$. Further reduction in the real frequency occurs in the fully nonlinear phase.

The evolution of vortices at the linear and nonlinear stages ($\Omega_i t > 160$) is shown in Figure 4. The electrostatic potential in the x-y plane has strong vortices at the center at $\Omega_i t = 240$. These vortices move along the direction of the $\mathbf{E} \times \mathbf{B}$ drift. As shown in Figure 4, the excited waves are well localized around the center. In the later nonlinear stage the number of the vortices is increased and one of the vortices migrates outward from the center.

The diffusion of the guiding center of ions in the case of the combination of TLE and FAC is shown at $\Omega_i t = 0$, 80, 160, 240, and 320 in Figure 5. A subset of ions with initial positions such that $58 \leq x \leq 64$, are followed in time, and the local guiding centers of ions are plotted at each time.

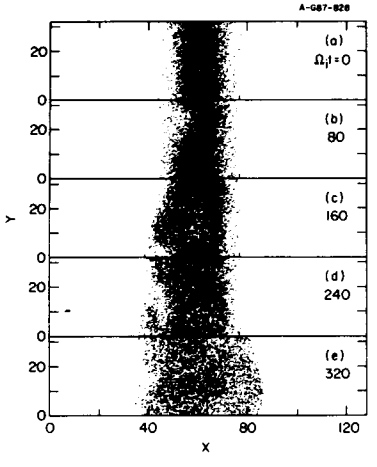

Figure 5. The diffusion of the gyro-center of ions whose initial actual positions are $58 \leq x \leq 64$ at $\Omega_i t = 0$, 80, 160, 240, and 320.

At the time ($\Omega_i t = 160$) when the waves begin to grow out of the thermal noise, slight waving of the column is observed. At the beginning of the nonlinear stage $\Omega_i t \simeq 240$, the column is twisted. In the nonlinear stage we see strong diffusion of the ions.

The local electric fields $E_{x,y}$ at $x = 74$, $y = 14$ is diagnosed, and the power spectrum is obtained.

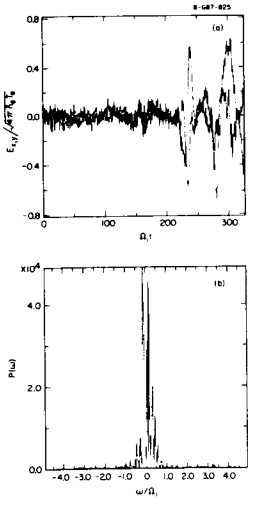

Figure 6. The time evolution of local electric field $E_{x,y}$ at $x = 74$, $y = 14$ (a) and its power spectrum (b).

As shown in Figure 6 (a), around $\Omega_i t = 230$ sharp peaks are produced. The spectrum has several peaks around $0.4\Omega_i$ which correspond to the real frequencies in the linear stage. The largest peak is produced by the vortices in the nonlinear stage.

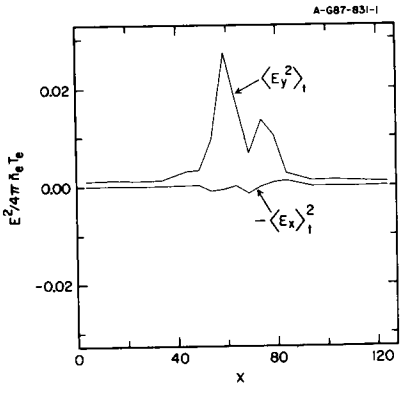

Figure 7. The average field energy $\langle E_y^2 \rangle_t$ and the d.c. type polarized electric field energy $-\langle E_x \rangle_t^2$ are localized around the center of the system.

The profiles of overall wave energy are shown in Figure 7. The time-averaged excited wave energy $\langle E_y^2 \rangle_t$ is localized around the center of the system. Obviously the excited wave energy is much larger than the thermal energy outside the electric field region. The time-averaged polarization electric field energy with minus sign $-\langle E_x \rangle_t^2$ is also plotted, which is much smaller than the excited wave energy.

3. DISCUSSIONS

We have investigated the electrostatic waves driven by the combined effects of a localized transverse electric field and parallel electron drifts by means of simulation with the assistance of the nonlocal kinetic theory (Ref. 12).

We have performed a number of simulations for this instability. Simulation results show that electrostatic waves are excited in the regions where the $\mathbf{E} \times \mathbf{B}$ drift is localized in the simultaneous presence of parallel electron drifts and transverse electric fields as predicted (Ref. 12). The magnitudes of the FAC and the TLE were chosen to be individually subcritical so that simulations with the FAC or the TLE when considered in isolation shows no instability, but when the combination is considered we find clear signatures of a growing wave. The physical mechanism underlying this instability is elucidated in the companion paper (Rerf. 12).

The nonlinear phenomena such as diffusion and coalescence of vortices are investigated. In the linear stage, smaller vortices are generated and larger vortices with the lower frequencies are dominant in the nonlinear stage. In the nonlinear stage the ions diffuse strongly due to the large scale vortices.

Our simulation results may explain the excitation of electrostatic waves of the observations (Ref. 2-4). However, more simulations are necessary to explain various other features of the observations. We are currently improving our simulation code to include the neutral-species collisions which are essential for the lower auroral region studies.

ACKNOWLEDGEMENTS

This research was supported by the National Aeronautics and Space Administration grant NGW-1239, National Science Foundation grant ATM-8519528, and Office of Naval Research Contracts Nos. N00173-87-M-4338 and N00014-88-K-2007. The simulations were performed on the CRAY X-MP48 at the National Center for Supercomputing Applications, University of Illinois at Urbana-Champaign, which is supported by the National Science Foundation.

REFERENCES

1. J. LaBelle, P. M. Kintner, A. W. Yau, and B. A. Whalen, J. Geophys. Res., **91**, 7113 (1986).

2. Sunanda Basu, Santimay Basu, C. Senior, D. Weimer, E. Nielsen, and P. F. Fougere, Geophys. Res. Lett., **13**, 101 (1986).

3. Sunanda Basu, Santimay Basu, E. MacKenzie, P. F. Fougere, W. R. Coley, N. C. Maynard, J. D. Winningham, M. Sugiura, W. B. Hanson, and W. R. Hoegy, J. Geophys. Res., **93**, 115 (1988).

4. G. D. Earle, Ph.D. Thesis, Cornell University, Ithaca, New York (1988).

5. P. Prikryl, D. Andre, G. J. Sofko, J. A. Koehler, and M. J. McKibben, Geophys. Res. Lett., **15**, 557 (1988).

6. W. E. Drummond and M. N. Rosenbluth, Phys. Fluids, **5**, 1507 (1962).

7. G. Ganguli, Y. C. Lee, and P. Palmadesso, Phys. Fluids, **28**,761, (1985).

8. G. Ganguli, P. Palmadesso, and Y. C. Lee, Geophys. Res. Lett., **12**, 643 (1985).

9. G. Ganguli, Y. C. Lee, and P. J. Palmadesso, Phys. Fluids, **31**, 823 (1988).

10. K.-I. Nishikawa, G. Ganguli, Y. C. Lee, and P. J. Palmadesso, Phys. Fluids, **31**, 1568 (1988).

11. G. Ganguli and P. Palmadesso, Geophys. Res. Lett., **15**, 103 (1988).

12. G. Ganguli, Y. C. Lee, P. J. Palmadesso, and S. L. Ossakow, submitted to the Proceeding of 1988 Cambridge Workshop in Theoretical Geoplasma Physics, (1988).

13. P. Prikryl, D. Andre, G.J. Sofko, J.A. Koehler, and M.J. McKibben, Geophys. Res. Lett., 15, 557 (1988)